HAL
open science

Propagation patterns in motor neuron diseases: Individual and phenotype-associated disease-burden trajectories across the UMN-LMN spectrum of MNDs

Marlene Tahedl, Stacey Li Hi Shing, Eoin Finegan, Rangariroyashe H Chipika, Jasmin Lope, Orla Hardiman, Peter Bede

To cite this version:

Marlene Tahedl, Stacey Li Hi Shing, Eoin Finegan, Rangariroyashe H Chipika, Jasmin Lope, et al.. Propagation patterns in motor neuron diseases: Individual and phenotype-associated disease-burden trajectories across the UMN-LMN spectrum of MNDs. Neurobiology of Aging, 2022, 109, pp.78-87. 10.1016/j.neurobiolaging.2021.04.031 . hal-03385140

HAL Id: hal-03385140

https://hal.sorbonne-universite.fr/hal-03385140

Submitted on 19 Oct 2021

HAL is a multi-disciplinary open access archive for the deposit and dissemination of scientific research documents, whether they are published or not. The documents may come from teaching and research institutions in France or abroad, or from public or private research centers.

L'archive ouverte pluridisciplinaire **HAL**, est destinée au dépôt et à la diffusion de documents scientifiques de niveau recherche, publiés ou non, émanant des établissements d'enseignement et de recherche français ou étrangers, des laboratoires publics ou privés.

Neurobiology of Aging 109 (2022) 78–87

Contents lists available at ScienceDirect

Neurobiology of Aging

journal homepage: www.elsevier.com/locate/neuaging.org

Propagation patterns in motor neuron diseases: Individual and phenotype-associated disease-burden trajectories across the UMN-LMN spectrum of MNDs

Marlene Tahedl[a,b,1], Stacey Li Hi Shing[a,1], Eoin Finegan[a,1], Rangariroyashe H. Chipika[a], Jasmin Lope[a], Orla Hardiman[a], Peter Bede[a,c,*]

[a] Computational Neuroimaging Group, Biomedical Sciences Institute, Trinity College Dublin, Ireland
[b] Department of Psychiatry and Psychotherapy and Institute for Psychology, University of Regensburg, 93053 Regensburg, Germany
[c] Pitié-Salpêtrière University Hospital, Sorbonne University, Paris, France

ARTICLE INFO

Article history:
Received 18 January 2021
Revised 29 March 2021
Accepted 13 April 2021
Available online 8 October 2021

Keywords:
Motor neuron disease
Primary lateral sclerosis
Poliomyelitis
Neuroimaging
Clinical trials

ABSTRACT

Motor neuron diseases encompass a divergent group of conditions with considerable differences in clinical manifestations, survival, and genetic vulnerability. One of the key aspects of clinical heterogeneity is the preferential involvement of upper (UMN) and lower motor neurons (LMN). While longitudinal imaging patters are relatively well characterized in ALS, progressive cortical changes in UMN,- and LMN-predominant conditions are seldom evaluated. Accordingly, the objective of this study is the juxtaposition of longitudinal trajectories in 3 motor neuron phenotypes; a UMN-predominant syndrome (PLS), a mixed UMN-LMN condition (ALS), and a lower motor neuron condition (poliomyelitis survivors). A standardized imaging protocol was implemented in a prospective, multi-timepoint longitudinal study with a uniform follow-up interval of 4 months. Forty-five poliomyelitis survivors, 61 patients with amyotrophic lateral sclerosis (ALS), and 23 patients with primary lateral sclerosis (PLS) were included. Cortical thickness alterations were evaluated in a dual analysis pipeline, using standard cortical thickness analyses, and a z-score-based individualized approach. Our results indicate that PLS patients exhibit rapidly progressive cortical thinning primarily in motor regions; ALS patients show cortical atrophy in both motor and extra-motor regions, while poliomyelitis survivors exhibit cortical thickness gains in a number of cerebral regions. Our findings suggest that dynamic cortical changes in motor neuron diseases may depend on relative UMN and/or LMN involvement, and increased cortical thickness in LMN-predominant conditions may represent compensatory, adaptive processes.

© 2021 The Author(s). Published by Elsevier Inc.
This is an open access article under the CC BY-NC-ND license
(http://creativecommons.org/licenses/by-nc-nd/4.0/)

Abbreviations: ACC, anterior cingulate cortex; ALS, amyotrophic lateral sclerosis; ALSFRS-r, revised amyotrophic lateral sclerosis functional rating scale; ANOVA, analysis of variance; ANCOVA, analysis of covariance; CC, corpus callosum; CIFTI, Connectivity Informatics Technology Initiative; CST, corticospinal tract; CT, cortical thickness; DTI, Diffusion Tensor Imaging; DV, dependent variable; EMM, estimated marginal mean; FOV, field of view; FWE, familywise error; FWER, family-wise error rates; GM, gray matter; HC, healthy control; HSD, Tukey's honestly significant difference; HSP, hereditary spastic paraplegia; IR-SPGR, inversion recovery prepared spoiled gradient recalled echo; IR-TSE, inversion recovery turbo spin echo; Lt, left; LL, Lower limb; LMN, lower motor neuron; MNI152, Montreal Neurological Institute 152 standard space; PCC, posterior cingulate cortex; PLS, primary lateral sclerosis; PMS, poliomyelitis survivors; Rt, right; ROI, region of interest; SBMA, spinal and bulbar muscular atrophy; SD, standard deviation; SE-EPI, spin-echo echo planar imaging; SENSE, Sensitivity Encoding; SMA, Spinal muscular atrophy; SPIR, spectral presaturation with inversion recovery; T1w, T1-weighted imaging; TE, Echo time; TFCE, threshold-free cluster enhancement; TI, Inversion time; TIV, total intracranial volume; TR, repetition time; UL, Upper limb; UMN, Upper motor neuron.

* Corresponding author at: Room 5.43, Computational Neuroimaging Group, Trinity Biomedical Sciences Institute, Trinity College Dublin, Pearse Street, Dublin 2, Ireland
E-mail address: bedep@tcd.ie (P. Bede).

[1] Contributed equally as joint first authors.

0197-4580/$ – see front matter © 2021 The Author(s). Published by Elsevier Inc. This is an open access article under the CC BY-NC-ND license (http://creativecommons.org/licenses/by-nc-nd/4.0/)
https://doi.org/10.1016/j.neurobiolaging.2021.04.031

1. Introduction

Motor neuron disease (MND) is an umbrella term for a wide spectrum of clinically dissimilar conditions. While similarities exist in disability profiles, progression rates and the overall prognosis is markedly different in various MNDs. Compared to ALS, other MNDs are strikingly understudied with respect to their phenotype-specific neuroimaging signatures. PLS and ALS groups are sometimes contrasted to each other to highlight disease-specific traits, (Pioro, et al., 2020) but lower motor neuron predominant MNDs, such as X-linked spinal, and bulbar atrophy (SBMA), poliomyelitis or spinal muscular atrophy (SMA) are typically only studied in contrast to healthy controls. (Li Hi Shing, et al., 2019, Querin, et al., 2018a) The imaging literature of MNDs is disproportionately dominated by cross-sectional studies which often include mixed cohorts in various stages in their individual disease course. Longitudinal studies of MND invariably suffer from considerable attrition rates and an inclusion bias to patients with limited disability and slower progression rates. (Chipika, et al., 2019) The meaningful interpretation of longitudinal imaging data requires careful adjustments for physiological aging, sexual-dimorphism, and ideally, the inclusion of disease-controls. (Schuster, et al., 2015) From a clinical perspective, there is a pressing and unmet need to monitor individual patients in a transparent and observer-independent fashion. (Tahedl, et al., 2021, Verstraete, et al., 2015) From a monitoring standpoint, a stereotyped question asked by patients and their caregivers is whether their condition have progressed since their previous clinic visit, irrespective of other patients, other phenotypes, or age-matched healthy populations. From a clinical trial perspective, the objective tracking of individual patients is a key requirement, preferably with the use of quantitative outcome measures. (Chipika, et al., 2019) Accordingly, the development of methods to track pathology in vivo, at an individual-patient level, is a hugely relevant quest. The characterisation of individual disease trajectories is also important academically. There are a number of emerging concepts in MND research, which are merely derived from post mortem findings, inferred from clinical observations or based on animal models, and have not been reassuringly validated by in vivo human data. These theories include cognitive reserve, motor reserve, stage-wise propagation, compensatory processes, prion-like propagation, and selective network vulnerability. (Costello, et al., 2021, Dukic, et al., 2019, Meier, et al., 2020) There is also a notion that compensatory processes may occur in MNDs to adapt for relentless neurodegeneration. (Querin, et al., 2019b) Activation studies in ALS suggest that the pre-, supplementary- and ipsilateral motor cortex, the cerebellum, and subcortical gray matter structures increasingly contribute to the execution of motor tasks with the gradual degeneration of primary motor areas. (Abidi, et al., 2020a, Bede, et al., 2021, Nasseroleslami, et al., 2019, Proudfoot, et al., 2018) Irrespective of the MND phenotype studied, the overwhelming majority of published papers only comment on patterns of atrophy, cortical thinning, or density reductions. (Bede and Hardiman, 2018) Lack of atrophy or 'resilient' regions are sometimes specifically evaluated, but increased cortical thickness is either not explored in statistical models, not reported, or not discussed. This seems like a missed opportunity as cortical reorganization may reveal biologically important processes. (Hardiman, et al., 2016) Based on these considerations, we have embarked on a comparative neuroimaging project to contrast the longitudinal course of three MNDs; a lower-motor predominant condition (poliomyelitis survivors), a mixed UMN-LMN syndrome (ALS), and a UMN-predominant condition (PLS). Our main objectives were (1) the characterization of phenotype-specific propagation patterns (2) the juxtaposition of the rate of decline in LMN, UMN and mixed MNDs and (3) the targeted evaluation of increased thickness.

2. Methods

2.1. Participants

Forty-five poliomyelitis survivors (PMS), 23 patients with PLS and 61 patients with ALS were included in a prospective neuroimaging study. Twenty-seven ALS patients had 2, 34 had 3 follow-up scans; 14 PMS had 1, 6 had 2 follow-up scans; 7 PLS patients had 2, 16 had 3 follow-up scans. A uniform inter-scan interval of 4 months was implemented. All participants provided informed consent in accordance with the ethics approval of the study by the Medical Research Committee of Beaumont Hospital, Dublin, Ireland. ALS patients had 'probable' or 'definite' ALS according to the El Escorial criteria (Brooks, et al., 2000) and PLS patients were diagnosed based on the Gordon criteria. (Gordon, et al., 2006) Reference data from 776 healthy control subjects were included (383 males) in our analyses (125 from Dublin, 651 from the Cam-CAN database, (Shafto, et al., 2014) with a mean age of 55.08 years and a standard deviation (SD) of 17.63 years.

2.2. Neuroimaging

T1-weighted (T1w) MRI data from all patients and controls was acquired on a 3 Tesla Philips Achieva scanner with an 8-channel receiver head coil, using a 3D Inversion Recovery Prepared Spoiled Gradient Recalled Echo (IR-SPGR) pulse sequence with following imaging parameters; repetition time (TR) / echo time (TE) = 8.5/3.9 ms, inversion time (TI) = 1060 ms, field-of-view (FOV): 256 × 256 × 160 mm, spatial resolution: 1 mm^3. A total of 651 external reference T1-weighted MPRAGE images were also used in this study from the Cambridge Centre for Ageing and Neuroscience (Cam-CAN) repository. (Shafto, et al., 2014)

2.3. Standard cortical thickness analysis

T1w datasets were segmented and the surface reconstructed with FreeSurfer's *recon-all* tool. (Fischl, 2012) Data were then converted to the Connecitivty Informatics Technology Initiative (CIFTI) file format (Van Essen, et al., 2013) using the CIFTIFY toolbox (Dickie, et al., 2019) at a resolution of 32,000 vertices per hemisphere. As part of 'standard' cortical thickness analyses, 3 group comparisons were performed (PMS vs. HC, ALS vs. HC, PLS vs. HC) using vertexwise, non–parametric permutation testing using FSLs *randomize* tool with 5000 iterations, controlling for age, and gender. (Winkler, et al., 2014) To correct for alpha-level inflation, we considered threshold-free cluster enhancement (TFCE) corrected p-maps only. (Salimi-Khorshidi, et al., 2011) Since we investigated 2 contrasts for each comparison (patients > controls, patients < controls), the alpha threshold was set to 0.05/2 = 0.025.

2.4. Normalized, 'mosaic-based' interpretation

'Standard' cortical thickness (CT) analyses were complemented by a z-score-based approach (Tahedl, 2020, Tahedl, et al., 2021) where regional cortical thickness in single patients is interpreted with respect to demographically matched controls, categorizing each cortical region ('mosaic') into 'thin,' 'thick' or 'comparable.' (Fig. 2 *for examples)* Following pre-processing, CT maps were parcellated into 1000 equally sized 'mosaics' using an existing parcellation scheme (Schaefer, et al., 2018) and implementing a 7-network approach. (Yeo, et al., 2011) A subject-specific reference group was generated for each patient based on age (+/– 2 years)

and gender matching. To account for the effects of physiological ageing a 'sliding-window' reference matching was implemented. For example, for a 56-year-old male patient, his control group comprised male controls aged between 54, and 58 years. At 1-year follow-up, his reference group shifted to male controls between 55, and 59 years. Regional cortical thickness in single patients was interpreted based on the CT distribution of demographically matched controls. Individual patient's regional thickness was first z-scored by subtracting the control's mean and dividing by the control's standard deviation. Subsequently, z-values are converted to *p*-values by exhaustive permutation testing to obtain FWER corrected *p*-values. A threshold of $p \leq 0.05$ was used to define 'thick' or 'thin.' The main output variables from the 'mosaic approach' are the number of significantly thin and thick patches across the entire cortex and in the motor, cortex defined by the pre- and paracentral labels of the Desikan-Killiany atlas. (Desikan, et al., 2006) To infer which patches were significantly thin or thick in the groups at baseline, Monte-Carlo permutation testing was used to correct for family-wise error rates (FWER), separately for the 3 study groups as well as for thin, and thick patches. The alpha-threshold was set to 0.025 to account for 2-sided testing. The analyses were conducted in MATLAB 2019b (The Mathworks, Natrick, MA, USA).

2.5. Cross-sectional group comparisons

As demographic matching is inherent in the 'mosaic' method, 1-way, 3-level, between-subjects analyses of variance (ANOVAs) was utilized to investigate group differences (PMS, ALS, and PLS) of the means of the following 4 dependent variables (DVs): (1) number of whole-brain thin patches, (2) number of motor-cortex thin patches, (3) number of whole-brain thick patches, (4) number of motor-cortex thick patches. For (5) whole-brain cortical thickness (CT) in millimeters and (6) motor-cortex CT in millimeters, analyses of covariance (ANCOVA) were utilized to correct for age, and gender. As the ANOVAs and ANCOVAs reached significance for 6 DVs, post-hoc pairwise comparisons were conducted using Tukey's honestly significant difference (HSD) testing. Statistical analyses were carried out with RStudio version 1.3.1093 (R Core Team, R Foundation for Statistical Computing, Vienna, Austria).

2.6. Longitudinal analyses using linear mixed effects models

To evaluate progressive cortical thickness alterations with the 'mosaic' approach, linear mixed effects (LME) models were implemented using Rs *nmle* package (Pinheiro et al., 2020):

(1) mod <- lme(DV ~ Time*Diagnosis, random =~ Time | ID, data = X , method = 'ML')

DV denotes the dependent variable, which is modelled as dependent upon the factor 'Time' and the categorical variable 'Diagnosis' (PMS / ALS / PLS). ID indicates the timepoint, which serves as a nested variable, since in longitudinal analyses data is per definition nested by individuals. Finally, X is the data containing information on all the specified variables. The method we used for estimating the model was maximum likelihood, 'ML'.

Given that in the standard approach (cortical thickness in millimeters), age and gender are not inherently corrected for, we set up these models as follows:

(2) mod2 <- lme(DV ~ Time*Diagnosis + age + gender, random =~ Time | ID, data = X , method = 'ML')

Although the LMEs captured no significant 'Time x Diagnosis' interaction, visual representation of the data (Fig. 5A and B) suggested that PLS patients accumulated thin patches more rapidly than the other patient groups. Since the data suggested this effect may be driven by the 1-year follow-up of the PLS patients, a supplementary 'Time x Diagnosis' LME analysis was added, restricted only to the baseline, and 1-year follow-up data.

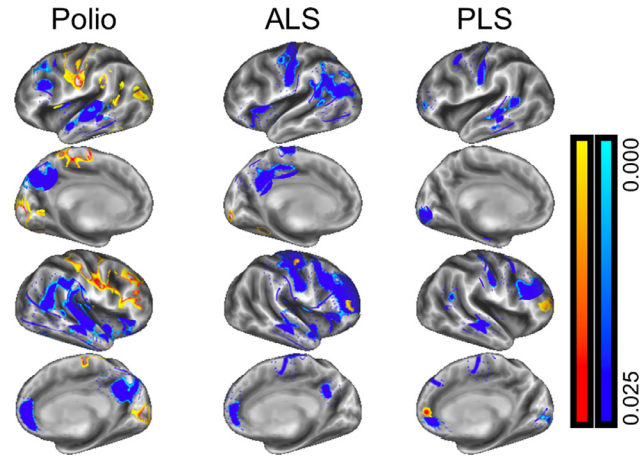

Fig. 1. Cortical thickness patterns based on vertexlwise permutation testing and corrections for age and gender in poliomyelitis survivors (left column), ALS (middle column) and PLS patients (right column).

3. Results

A total of 776 healthy control subjects (383 males) were included in our analyses (125 from Dublin, 651 from the Cam-CAN database, with a mean age of 55.08 years (SD: 17.63y). The mean age of the 45 PMS patients (20 males) at baseline was 66.07 years (+/−6.52), the mean interval between their acute poliomyelitis infection in infancy, and their initial brain scan was 62.75 years. The mean age of the 61 ALS patients (43 males) was 60.20 (+/− 9.62 years), and their mean symptom duration was 43 months. The age profile of the 23 PLS patients (12 males) was 58.52 years (+/− 9.79 years) and mean symptom duration 52 months. In accordance with the demographic matching procedure, (Tahedl, et al., 2021) 82 individualized reference groups were generated. The cross-sectional comparisons of CT maps between PMS patients and HCs (Fig. 1) revealed significant cortical thinning of the bilateral superior temporal gyri, the bilateral medial posterior cingulate cortices (PCC), the right anterior cingulate cortex (ACC), and parts of the left frontal cortex. Intriguingly, we observed increased thickness in the bilateral sensorimotor cortices, as well as parts of the bilateral medial visual cortices and the right frontal cortex. In ALS patients, cortical thinning was most evident in the bilateral motor cortices, left frontal and bilateral temporal cortices, as well as bilateral PCC and right ACC. Small regions of thicker cortex were also observed in the right pre- and frontal cortices. In PLS, cortical thinning was most evident in the bilateral motor cortices as well as widespread frontotemporal regions. Small regions of thicker cortex were observed in the right rostral middle frontal and the right medial orbitofrontal cortex. The mosaic-based CT analysis resulted in individual subject brain maps, indicating regional cortical changes with respect to subject-matched controls. Representative patient maps are shown in Fig. 2 to illustrate individual cortical patterns across the timepoints.

3.1. Inferential statistics of the mosaic brain maps

Permutation testing was used to infer which cortical regions were significantly 'thin' or 'thick' in each phenotype. As illustrated in Fig. 3, PMS patients exhibit 'thick' patches (red-yellow) around

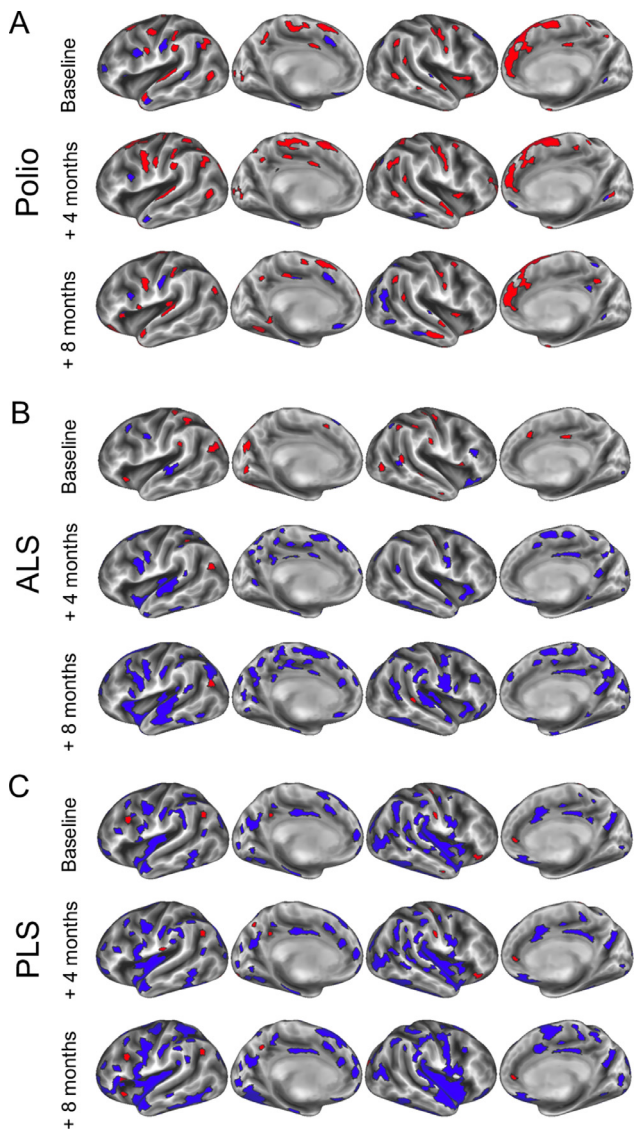

Fig. 2. The 'mosaic-based' approach permits the evaluation of individual patient scans with respect to age-and gender matched controls. 'Thin' regions are color-coded in blue and 'thick' regions in red. Representative examples of individual patients are shown at baseline and follow-ups in (A) a poliomyelitis survivor (B) ALS patient and (C) a PLS patient (Color version of the figure is available online.)

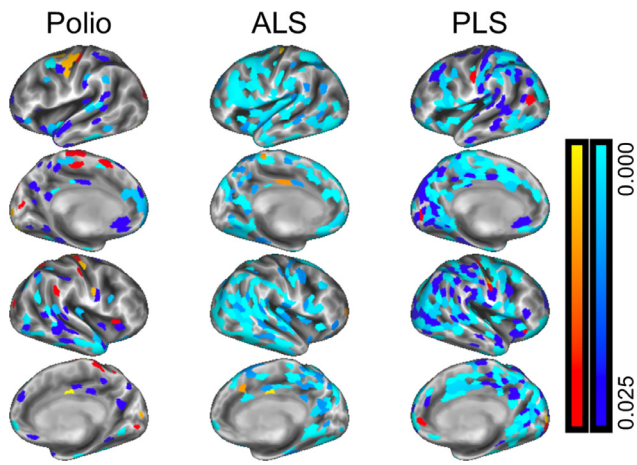

Fig. 3. Baseline cortical characteristics in poliomyelitis survivors (left column), ALS (middle column) and PLS using the 'mosaic approach.'

the bilateral sensorimotor cortices. A cluster of atrophic patches (blue-light blue) was observed in the right temporal cortex, in addition to thin patches scattered across the cortex. In ALS and PLS, atrophic patches dominate the entire cortical surface, with only occasional 'thick' patches observed in middle frontal, and inferior precentral areas in PLS.

3.2. Cross-sectional group comparisons

Significant cross-sectional differences were noted in all 6 dependent variables (Fig. 4 *A–F*): (1) whole-brain thin patches (F[2] = 24.51, p = 1.02e-09), (2) motor-cortex thin patches (F[2] = 38.16, p = 1.1e-13), (3) whole-brain thick patches (F[2] = 6.468, p = 0.0021), (4) motor-cortex thick patches (F[2] = 7.717, p = 6.9e-04), (5) whole-brain thickness (F[2] = 20.20, p_{corr} = 2.55e-08), and (6) motor-cortex thickness (F[2] = 32.50, p_{corr} = 4.482e-12). Post-hoc Tukey's HSD confirmed differences in the following pairwise comparisons at $p < 0.05$: (1) whole-brain thin patches: PMS (mean 56.07, SD 46.92) < ALS (98.90 +/– 87.64) (p = 0.02061), PMS < PLS (200 +/– 107.77) (p = 0.0000), and ALS < PLS (p = 3.0e-06); (2) motor-cortex thin patches: PMS (5.62 +/– 4.69) < ALS (14.43 +/– 14.74) (p = 0.0022), PMS < PLS (34.65 +/– 18.12) (p = 0.0000) and ALS < PLS (p = 0.0000); (3) whole-brain thick patches: PMS (31.53 +/– 33.97) > PLS (9.7 +/– 9.09) (p = 0.0016); (4) motor-cortex thick patches: PMS (7.27 +/– 6.81) > ALS (4.51 +/– 4.76) (p = 0.0261), PMS > PLS (2.09 +/– 3.03) (p = 0.0007); (5) whole-brain thickness: PMS (2.34 mm +/– 0.09 mm) > PLS (2.2 mm +/– 0.11 mm) (p_{corr} = 1.8e-06), ALS (2.31 mm +/– 0.11mm) > PLS (p_{corr} = 0.0001); (6) motor-cortex thickness: PMS (2.31 mm +/– 0.11mm) > ALS (2.25 mm +/– 0.13 mm) (p_{corr} = 0.0293), PMS > PLS (2.09 mm +/– 0.11 mm) (p_{corr} = 0.0000), ALS > PLS (p_{corr} = 5.0e-07).

3.3. Longitudinal analysis using linear mixed effects models

Longitudinal progression of the 6 DVs was evaluated using linear mixed effect models (Fig. 5*A–F*). We found that for thin patches and raw cortical thickness – but not for thick patches – the main effect "Time" was significant, showing an increase of the thin-patch count and a decrease of CT over time across the diagnoses groups [whole-brain thin patches: t(235) = 2.2956, p = 0.0226; motor-cortex thin patches: t(235) = 2.4767, p = 0.0140; whole-brain CT: t(234) = -4.1241, p_{corr} = 0.0000; motor-cortex CT: t(234) = -5.1505, p_{corr} = 0.0000). Additionally, we found a main effect "Diagnosis" for the thin-patch count (Fig. 5A and B), separating both PMS and PLS from ALS, both for the whole-brain as well as the restricted motor-cortex count (whole-brain PLS: t(126) = 4.1607, p = 0.0001; whole-brain PMS: t(126) = -2.5651, p = 0.0115; motor-cortex PMS: t(126) = -3.1327, p = 0.0022; motor-cortex PLS: t(126) = 5.4094, p = 0.0000). In contrast, for the thick-patch count (Fig. 5C and D), we observed no main effect of time, and in terms of the main effect of diagnosis, only the PMS group differed from the ALS group (whole-brain: t[126] = 2.1188, p = 0.0361; motor-cortex: t[126] = 2.8325, p = 0.0054). For the standard approach (Fig. 5E and F), the main effect "Diagnosis" was evident for PMS versus ALS patients (t[125] = 2.9811, p_{corr} = 0.0035), as well as PLS versus ALS patients for the whole-brain analysis (t[125] = -3.8097, p_{corr} = 0.0002); likewise for the restricted motor-cortex analysis, both PMS and PLS patients differed from ALS (PMS vs. ALS: t(125) = 3.8037, p_{corr} = 0.0002; PLS vs. ALS: t(125) = -4.9094, p_{corr} = 0.0000). Given the differences in the available follow-up scans in the different study groups, a supplementary analysis was conducted only taking into account the baseline and 1-year follow-up data in PLS and ALS patients. This LME revealed significant interaction effects of Time x Diagnosis, for

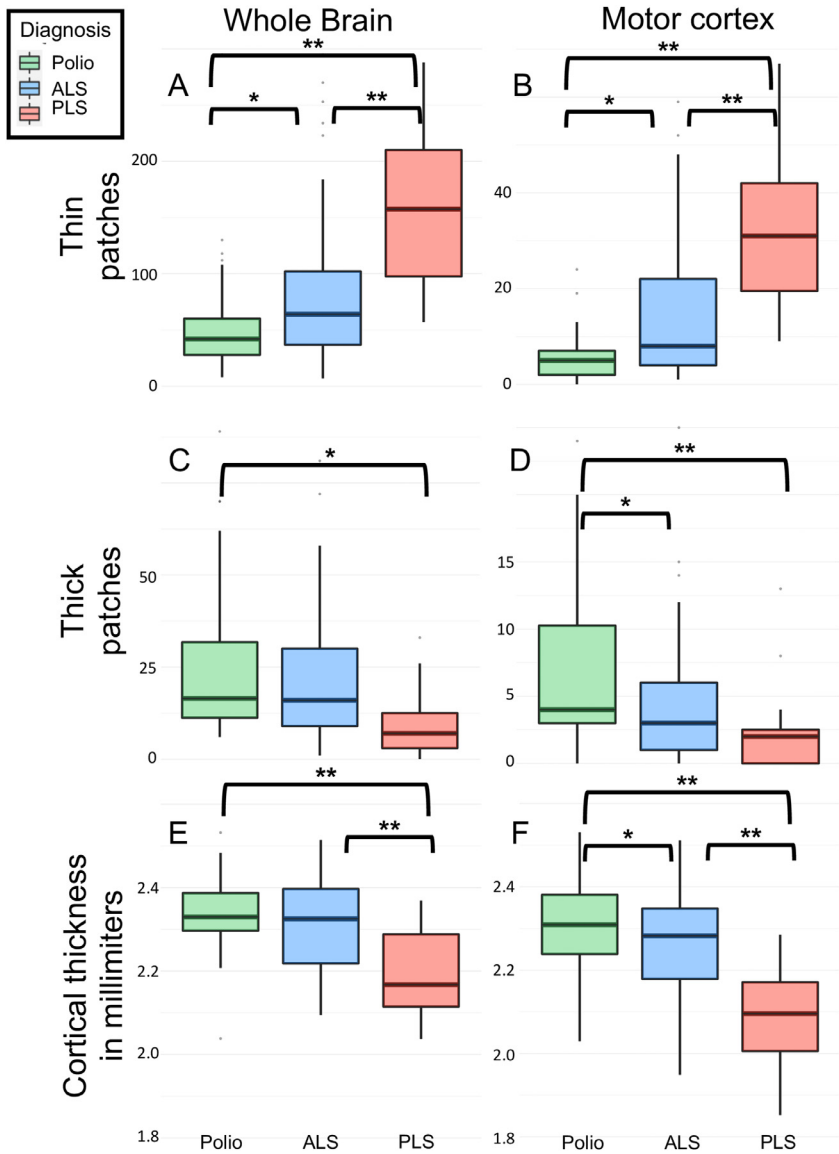

Fig. 4. Cortical thickness over the entire brain and in the motor cortex in poliomyelitis survivors (green), ALS (blue) and PLS (red). Box-plots represent the interquartile range and whiskers indicate IQRx1.5. Tukey's honestly significant difference testing was used for post-hoc pairwise comparisons: (*) indicates p-values < 0.05 (**) indicates p-values < 0.001 (Color version of the figure is available online.)

both whole-brain (t[48] = 2.3004, $p = 0.0258$) and motor-cortex-only (t[48] = 2.6795, $p = 0.0101$) thin-patch count. For standard CT values, whole-brain average CT revealed significant differences (t[48] = -2.4035, $p = 0.0202$), while the restricted motor-cortex analysis only approached significance (t[48] = -1.9350, $p = 0.0589$).

4. Discussion

Our findings indicate divergent cortical signatures in UMN-predominant, LMN-predominant and mixed UMN-LMN MND phenotypes. Our results also reveal co-existing atrophy and increased cortical thickness in MND, in both LMN- and UMN-predominant phenotypes. Additionally, our results confirm the feasibility of individual patient MRI interpretation using patient-specific normative data sets.

Longitudinal imaging in MND is one of the few ways to characterize progressive pathologic changes in vivo, to evaluate anatomical propagation patterns, verify concepts of disease-biology, and validate staging systems. (Chipika, et al., 2019, Müller, et al., 2020, Muller, et al., 2016) Longitudinal imaging studies have been published in symptomatic ALS patients and asymptomatic mutation carriers, but the majority of studies lacked 'disease-controls' and relied solely on healthy aging populations for data interpretation. (Querin, et al., 2019a) With few exceptions, (Clark, et al., 2017) no robust longitudinal studies have been published in PLS, despite the long course and relatively good prognosis associated with the condition. Based on clinical observations, there is a notion that PLS may be slowly progressive compared to ALS, but no robust quantitative imaging studies exist to support this notion. (Finegan, et al., 2019b) Recent post-mortem studies confirmed both motor cortex and extra-motor TDP-43 pathology in PLS (Mackenzie and Briemberg, 2020) and neuropsychology studies also highlighted considerable cognitive deficits. (de Vries, et al., 2019) It is increasingly recognized that similarly to ALS, (Burke, et al., 2016) PLS is also associated with considerable extra-motor manifestations.(Finegan, et al., 2021)

Imaging studies in PLS have largely revealed comparable cerebral signatures in ALS and PLS with the shared involvement

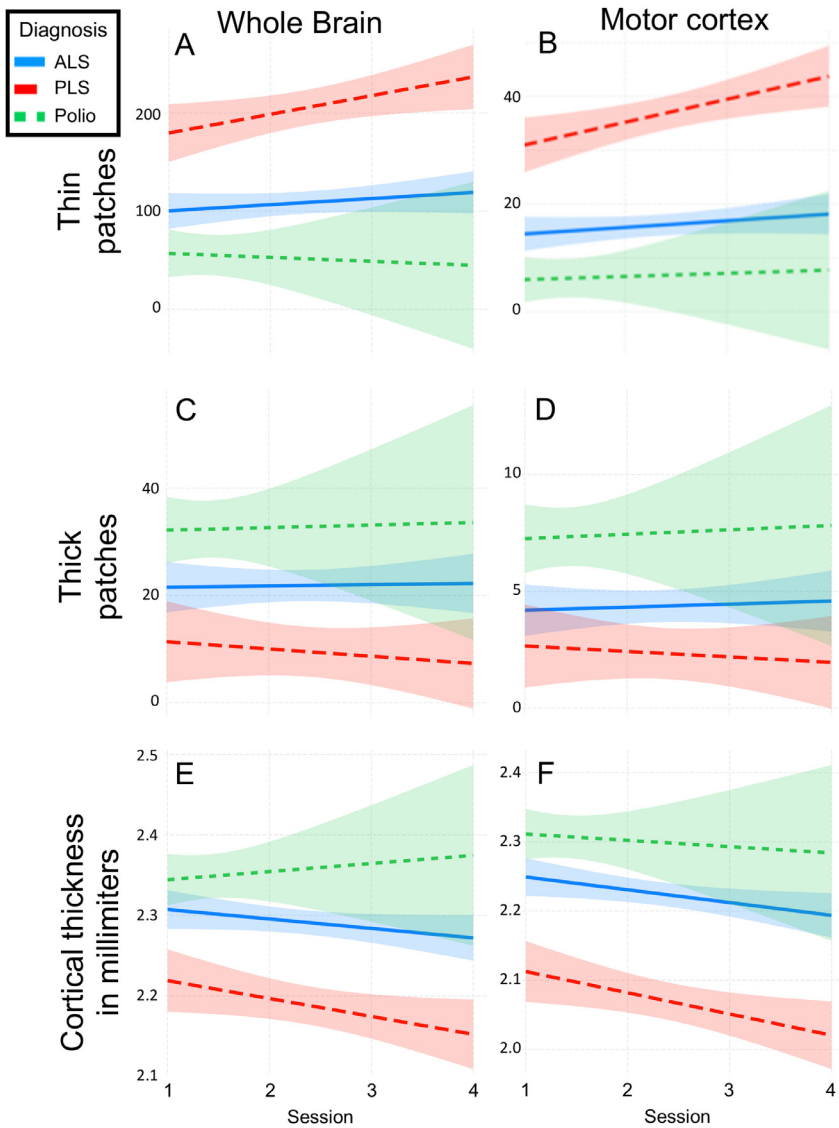

Fig. 5. Linear mixed effects models confirming that for all dependent variables are associated with cortical thinning (A, B, E, F), time was a significant predictor of worsening. In contrast, hypertrophy (C and D) was stable over time, showing only a main effect of "Diagnosis" with respect to the poliomyelitis survivors. Lines denote the best-fit line of the regressions, the shadowed area around the lines indicate 95% confidence intervals.

of the PMC, brainstem, cerebellum, CSTs, and CC. (Bede, et al., 2020, Bede, et al., 2019, Muller, et al., 2012, van der Graaff, et al., 2011a) Very few PLS studies identified distinguishing radiological changes from ALS; and these proposed that contrary to ALS, the postcentral gyrus may spared (Finegan, et al., 2019a) and the subcortical signature of PLS may be different from ALS. (Chipika, et al., 2020,E. Finegan, et al., 2020, Finegan, et al., 2019c) Some studies suggest greater PMC atrophy (Kiernan and Hudson, 1994, Menke, et al., 2018, van der Graaff, et al., 2010) and more marked CST degeneration in PLS (Agosta, et al., 2014, Van Der Graaff, et al., 2011b) than in ALS, but others have not replicated these findings. (Ferraro, et al., 2017, Müller, et al., 2018) Given the relative lack of convincing cross-sectional differences between ALS and PLS, longitudinal studies may be better suited to capture distinguishing features. (Christidi, et al., 2018) The distinction of PLS and ALS is hugely important in the first years of symptom onset, as there is often a diagnostic dilemma in early PLS, and an apprehension that a patient with UMN-predominant symptoms may transition to ALS. (Eoin Finegan, et al., 2020a, Eoin Finegan, et al., 2020b, Turner, et al., 2020, Yunusova, et al., 2019)

MNDs include a range of LMN-predominant conditions (Lebouteux, et al., 2014) including progressive muscular atrophy (PMA), Spinal muscular atrophy (SMA), Kennedy's disease (SBMA), progressive bulbar palsy (PBP), monomelic amyotrophy, flail arm and/or flail leg syndrome etc. (Hardiman, et al., 2016) The cerebral imaging literature of these syndromes is particularly scarce as the primary pathology is in the spinal anterior horns and the brainstem nuclei. (Li Hi Shing, et al., 2021) Recent PMA studies captured cervical spinal cord atrophy (van der Burgh, et al., 2019) without overt cerebral connectivity alterations. (Basaia, et al., 2020) Some PMA studies captured decreased cerebral white matter integrity (Prudlo, et al., 2012) and abnormal prefrontal activation patterns (Raaphorst, et al., 2014), while others did not detect FA reductions. (Cosottini, et al., 2005, Mitsumoto, et al., 2007) Tractography in a PMA cohort revealed FA reductions subjacent to the PMC with concomitant FA increase in the rostral internal capsule and/or corona radiata. (van der Graaff, et al., 2011a) Post mortem studies have

also captured corticospinal tract degeneration in patients labelled with PMA on clinical grounds (Ince, et al., 2003) casting doubt on whether PMA can be viewed as a distinct entity. Radiological reports of SBMA are just as conflicting. Cerebellar, pyramidal tract, and limbic white matter degeneration was described by some studies (Kassubek, et al., 2007, Pieper, et al., 2013, Unrath, et al., 2010), but not confirmed by others. (Echaniz-Laguna, et al., 2005, Nelles, et al., 2008, Spinelli, et al., 2019) Varying degree of frontal lobe atrophy (Sperfeld, et al., 2005) and hypometabolism (Lai, et al., 2013) have also been described. The biomarker literature of SMAs is dominated by electrophysiology studies, (Querin, et al., 2018c) and existing imaging studies are strikingly inconsistent. While cerebral changes have been described in SMA type 0, (Mendonça, et al., 2019) type II, (Losito, et al., 2020) and adult SMA variants, (de Borba, et al., 2020) other studies specifically highlight the lack of cerebral involvement despite considerable spinal cord degeneration. (Querin, et al., 2019b)

Our findings reveal distinct cortical signatures in LMN-predominant, UMN-predominant, and mixed MND phenotypes. The juxtaposition of the 3 phenotypes helps to highlight disease-specific traits. Poliomyelitis survivors exhibit increased cortical thickness in both motor and extra-motor regions revealing a unique imaging signature. This pattern is readily captured by both traditional cortical thickness analyses and the individualized 'mosaic-based' approach using subject-specific normative data. The co-existing patterns of cortical atrophy and cortical hypertrophy in poliomyelitis survivors showcases the importance of 2-way analyses in MND, and highlights the pitfalls of implementing hypothesis-aligned, 1-way contrasts only. The widespread regions showing increased cortical thickness in poliomyelitis survivors are reminiscent of other LMN conditions such as adult forms of SMA. (Querin, et al., 2019b) UMN-predominant MND patients were represented by a group of PLS patients in this study. Consistent with previous reports, they exhibit primary motor cortex (PMC) atrophy with additional frontotemporal involvement. It is noteworthy, that both at group-level, and at individual level, PLS patients also show regions of increased cortical thickness. The discussion around the interpretation of these findings is stimulating, as PLS is an archetypal neurodegenerative condition with considerable disability which is relatively well-characterized with regards to TDP-43 burden. (Mackenzie and Briemberg, 2020) Despite representing the opposing extremes of the LMN-UMN spectrum, a shared feature of PMS, and PLS is the realtively long survival which may permit compensatory processes to take place leading to structural reorganization. Adaptive cortical changes have been observed following spinal cord injuries, (Nishimura and Isa, 2009) in response to repetitive tasks, arduous physical training, dexterity associated with musical instruments, and association with cognitive training. Adaptive motor cortex changes have been consistently noted after unimanual training, (Sale, et al., 2017) aerobic exercise, (Colcombe, et al., 2006) post stroke, (Sterr, et al., 2013), and in professional musicians. (Bruchhage, et al., 2020, Gaser and Schlaug, 2003, Hudziak, et al., 2014) Extra-motor changes have also been observed following various exercise regimes, (Pereira, et al., 2007, Thomas, et al., 2016) and cognitive tasks. (Lazar, et al., 2005) Despite ample examples of cortical volume gains in a range of conditions, cortical thickness increases or volume gains are seldom evaluated or reported in MNDs. In the ALS cohort, we have not observed widespread hypertrophic regions which may be explained the shorter symptom duration of this cohort. Our findings also suggest that longitudinal imaging may be better suited to differentiate MND phenotypes than cross-sectional imaging, as propagation patterns, and rate of progression may be more specific to MND phenotypes than a snapshot of cortical disease burden.

The comparable cortical disease burden observed in PLS and ALS stands in stark contrast with the much shorter survival in ALS. Our longitudinal analyses also demonstrate faster cortical thinning in PLS than ALS. These observations suggest that cortical disease burden does not drive survival, and ALS patients are likely to succumb to the sequelae of LMN degeneration. While hypertrophic brain regions are seldom reported in ALS, unaffected regions have been specifically investigated. (Bede, et al., 2016) Furthermore, some ALS studies confirmed divergent imaging profiles between UMN-predominant, and LMN-predominant ALS patients. (Abidi, et al., 2020b) Even tough increased cortical thickness has not been reported in ALS, functional studies have consistently captured adaptive changes with the increasing involvement of cerebellar, subcortical, and contralateral motor regions in the execution of motor tasks. (Bede, et al., 2021, Proudfoot, et al., 2018).

We presented a z-score-based approach to interpret single-patient imaging data, but several other methods have been successfully explored in ALS. (Grollemund, et al., 2019) Wet biomarkers (Blasco, et al., 2018, Devos, et al., 2019), clinical parameters (Elamin, et al., 2015, Westeneng, et al., 2018) and MRI data (Bede et al., 2021, Querin, et al., 2018b, Welsh, et al., 2013) have been used in a variety of machine-learning applications to categorize single subjects into diagnostic (Bede, et al., 2017, Schuster, et al., 2016) or prognostic groups (Grollemund, et al., 2020a, Grollemund, et al., 2020b, Schuster, et al., 2017).

This study is not without limitations. Despite our dual-methodological approach, only cortical gray matter changes have been evaluated, and white matter integrity has not been assessed in this study. We have no supporting post mortem data to evaluate regions of increased cortical thickness and assess the histologic underpinnings of our imaging findings. Owing to the low incidence of PLS, we had a relatively limited sample size at our disposal. While physiological aging is accounted for in our 'mosaic' model by implementing a 'sliding window' approach, the availability of longitudinal control data would have permitted more fine-grained statistical modelling. The inclusion of additional LMN conditions may have helped to support our biological interpretation, namely that cerebral reorganization may occur in anterior horn pathologies. Despite these limitations we have demonstrated different cortical trajectories along the LMN-UMN spectrum of MNDs. We have also shown that cortical disease burden can not only be interrogated at a cohort-level but may also be meaningfully evaluated at an individual-level. Our study draws attention to areas of increased cortical thickness which are notoriously underevaluated in neurodegenerative conditions despite representing an important facet of disease biology.

5. Conclusions

The longitudinal analysis of cortical disease burden distinguishes MND phenotypes, which exhibit markedly differing trajectories. MND patients don't solely exhibit cortical atrophy, but LMN-phenotypes in particular, show regions of increased cortical thickness as well. These radiological changes may represent adaptive processes, may be indicative of neuroplasticity, but the post mortem correlates of regions of 'hypertrophy' remain to be elucidated. Our study demonstrates that cortical disease-burden may be interpreted at an individual-levelwhich is particularly useful in a clinical or clinical trial setting.

Authors' contribution

Conceptualization, Methodology, Imaging analyses, Drafting the manuscript: MT, PB. Investigation, Project administration, Revision for intellectual content: SLHS, EF, RHC, JL, OH, PB.

Funding

This study was sponsored by the Spastic Paraplegia Foundation, Inc (SPF). Professor Peter Bede and the computational neuroimaging group (CNG) are also supported by the Health Research Board (HRB EIA-2017-019), the EU Joint Programme – Neurodegenerative Disease Research (JPND), the Andrew Lydon scholarship, the Irish Institute of Clinical Neuroscience (IICN), and the Iris O'Brien Foundation. Marlene Tahedl is funded by the Deutsche Multiple Sklerose Gesellschaft (DMSG), grant number 2018-DMSG-08.

Disclosure statement

The authors have no actual or potential conflicts of interest.

Acknowledgements

We are most thankful for the participation of each patient and healthy control, and we also thank all the patients who expressed interest in this research study but were unable to participate for medical or logistical reasons. We also express our gratitude to the caregivers of MND patients for facilitating attendance at our neuroimaging center. Without their generosity this study would have not been possible.

References

Abidi, M., de Marco, G., Couillandre, A., Feron, M., Mseddi, E., Termoz, N., Querin, G., Pradat, P.F., Bede, P. 2020a. Adaptive functional reorganization in amyotrophic lateral sclerosis: coexisting degenerative and compensatory changes. Eur J Neurol 27(1), 121-8. doi:10.1111/ene.14042.

Abidi, M., de Marco, G., Grami, F., Termoz, N., Couillandre, A., Querin, G., Bede, P., Pradat, P.F., 2020b. Neural correlates of motor imagery of gait in amyotrophic lateral sclerosis. J Magn Reson Imaging doi:10.1002/jmri.27335.

Agosta, F., Galantucci, S., Riva, N., Chiò, A., Messina, S., Iannaccone, S., Calvo, A., Silani, V., Copetti, M., Falini, A., Comi, G., Filippi, M., 2014. Intrahemispheric and interhemispheric structural network abnormalities in PLS and ALS. Hum Brain Mapp 35 (4), 1710–1722. doi:10.1002/hbm.22286.

Basaia, S., Agosta, F., Cividini, C., Trojsi, F., Riva, N., Spinelli, E.G., Moglia, C., Femiano, C., Castelnovo, V., Canu, E., Falzone, Y., Monsurrò, M.R., Falini, A., Chiò, A., Tedeschi, G., Filippi, M., 2020. Structural and functional brain connectome in motor neuron diseases: a multicenter MRI study. Neurology 95 (18), e2552–e2e64. doi:10.1212/wnl.0000000000010731.

Bede, P., Bogdahn, U., Lope, J., Chang, K.M., Xirou, S., Christidi, F., 2021. Degenerative and regenerative processes in amyotrophic lateral sclerosis: motor reserve, adaptation and putative compensatory changes. Neural Regen Res 16 (6), 1208–1209. doi:10.4103/1673-5374.300440.

Bede, P., Chipika, R.H., Finegan, E., Li Hi Shing, S., Chang, K.M., Doherty, M.A., Hengeveld, J.C., Vajda, A., Hutchinson, S., Donaghy, C., McLaughlin, R.L., Hardiman, O., 2020. Progressive brainstem pathology in motor neuron diseases: Imaging data from amyotrophic lateral sclerosis and primary lateral sclerosis. Data Brief 29, 105229. doi:10.1016/j.dib.2020.105229.

Bede, P., Chipika, R.H., Finegan, E., Li Hi Shing, S., Doherty, M.A., Hengeveld, J.C., Vajda, A., Hutchinson, S., Donaghy, C., McLaughlin, R.L., Hardiman, O., 2019. Brainstem pathology in amyotrophic lateral sclerosis and primary lateral sclerosis: a longitudinal neuroimaging study. NeuroImage Clinical 24, 102054. doi:10.1016/j.nicl.2019.102054.

Bede, P., Hardiman, O., 2018. Longitudinal structural changes in ALS: a three time-point imaging study of white and gray matter degeneration. Amyotroph Lateral Scler Frontotemporal Degener 19 (3-4), 232–241. doi:10.1080/21678421.2017.1407795.

Bede, P., Iyer, P.M., Finegan, E., Omer, T., Hardiman, O., 2017. Virtual brain biopsies in amyotrophic lateral sclerosis: diagnostic classification based on in vivo pathological patterns. NeuroImage Clinical 15, 653–658. doi:10.1016/j.nicl.2017.06.010.

Bede, P., Iyer, P.M., Schuster, C., Elamin, M., McLaughlin, R.L., Kenna, K., Hardiman, O., 2016. The selective anatomical vulnerability of ALS: 'disease-defining' and 'disease-defying' brain regions. Amyotroph Lateral Scler Frontotemporal Degener 17 (7-8), 561–570. doi:10.3109/21678421.2016.1173702.

Bede, P., Murad, A., Hardiman, O., 2021. Pathological neural networks and artificial neural networks in ALS: diagnostic classification based on pathognomonic neuroimaging features. J Neurol doi:10.1007/s00415-021-10801-5.

Blasco, H., Patin, F., Descat, A., Garcon, G., Corcia, P., Gele, P., Lenglet, T., Bede, P., Meininger, V., Devos, D., Gossens, J.F., Pradat, P.F, 2018. A pharmacometabolomics approach in a clinical trial of ALS: Identification of predictive markers of progression. PLoS One 13 (6), e0198116. doi:10.1371/journal.pone.0198116.

Brooks, B.R., Miller, R.G., Swash, M., Munsat, T.LResearch Group on Motor Neuron Diseases, 2000. El Escorial revisited: revised criteria for the diagnosis of amyotrophic lateral sclerosis. Amyotroph Lateral Scler Other Motor Neuron Disord 1 (5), 293–299.

Bruchhage, M.M.K., Amad, A., Draper, S.B., Seidman, J., Lacerda, L., Laguna, P.L., Lowry, R.G., Wheeler, J., Robertson, A., Dell'Acqua, F., Smith, M.S., Williams, S.C.R, 2020. Drum training induces long-term plasticity in the cerebellum and connected cortical thickness. Sci Rep 10 (1), 10116. doi:10.1038/s41598-020-65877-2.

Burke, T., Pinto-Grau, M., Lonergan, K., Elamin, M., Bede, P., Costello, E., Hardiman, O., Pender, N., 2016. Measurement of social cognition in amyotrophic lateral sclerosis: a population based study. PLoS One 11 (8), e0160850. doi:10.1371/journal.pone.0160850.

Chipika, R.H., Finegan, E., Li Hi Shing, S., Hardiman, O., Bede, P., 2019. Tracking a fast-moving disease: longitudinal markers, monitoring, and clinical trial endpoints in ALS. Front Neurol 10, 229. doi:10.3389/fneur.2019.00229.

Chipika, R.H., Finegan, E., Li Hi Shing, S., McKenna, M.C., Christidi, F., Chang, K.M., Doherty, M.A., Hengeveld, J.C., Vajda, A., Pender, N., Hutchinson, S., Donaghy, C., McLaughlin, R.L., Hardiman, O., Bede, P., 2020. Switchboard" malfunction in motor neuron diseases: Selective pathology of thalamic nuclei in amyotrophic lateral sclerosis and primary lateral sclerosis. NeuroImage Clinical 27, 102300. doi:10.1016/j.nicl.2020.102300.

Christidi, F., Karavasilis, E., Rentzos, M., Kelekis, N., Evdokimidis, I., Bede, P., 2018. Clinical and radiological markers of extra-motor deficits in amyotrophic lateral sclerosis. Front Neurol 9, 1005. doi:10.3389/fneur.2018.01005.

Clark, M., Huang, C., Bageac, D., Danielian, L., Smallwoed, R., Floeter, M.K, 2017. Neuroimaging changes in the first 5 years of symptoms in patients with primary lateral sclerosis. Amyotroph Lateral Scler Frontotemporal Degener 18, 216–217. doi:10.1080/21678421.2017.1374605/008.

Colcombe, S.J., Erickson, K.I., Scalf, P.E., Kim, J.S., Prakash, R., McAuley, E., Elavsky, S., Marquez, D.X., Hu, L., Kramer, A.F, 2006. Aerobic exercise training increases brain volume in aging humans. J Gerontol A Biol Sci Med Sci 61 (11), 1166–1170. doi:10.1093/gerona/61.11.1166.

Cosottini, M., Giannelli, M., Siciliano, G., Lazzarotti, G., Michelassi, M.C., Del Corona, A., Bartolozzi, C., Murri, L, 2005. Diffusion-tensor MR imaging of corticospinal tract in amyotrophic lateral sclerosis and progressive muscular atrophy. Radiology 237 (1), 258–264. doi:10.1148/radiol.2371041506.

Costello, E., Rooney, J., Pinto-Grau, M., Burke, T., Elamin, M., Bede, P., McMackin, R., Dukic, S., Vajda, A., Heverin, M., Hardiman, O., Pender, N., 2021. Cognitive reserve in amyotrophic lateral sclerosis (ALS): a population-based longitudinal study. J Neurol Neurosurg Psychiatry doi:10.1136/jnnp-2020-324992.

de Borba, F.C., Querin, G., França Jr., M.C., Pradat, P.F, 2020. Cerebellar degeneration in adult spinal muscular atrophy patients. J Neurol 267 (9), 2625–2631. doi:10.1007/s00415-020-09875-4.

de Vries, B.S., Spreij, L.A., Rustemeijer, L.M.M., Bakker, L.A., Veldink, J.H., van den Berg, L.H., Nijboer, T.C.W., van Es, M.A., 2019. A neuropsychological and behavioral study of PLS. Amyotroph Lateral Scler Frontotemporal Degener 20 (5-6), 376–384. doi:10.1080/21678421.2019.1620284.

Desikan, R.S., Segonne, F., Fischl, B., Quinn, B.T., Dickerson, B.C., Blacker, D., Buckner, R.L., Dale, A.M., Maguire, R.P., Hyman, B.T., Albert, M.S., Killiany, R.J, 2006. An automated labeling system for subdividing the human cerebral cortex on MRI scans into gyral based regions of interest. NeuroImage 31 (3), 968–980. doi:10.1016/j.neuroimage.2006.01.021.

Devos, D., Moreau, C., Kyheng, M., Garcon, G., Rolland, A.S., Blasco, H., Gele, P., Timothee Lenglet, T., Veyrat-Durebex, C., Corcia, P., Dutheil, M., Bede, P., Jeromin, A., Oeckl, P., Otto, M., Meninger, V., Danel-Brunaud, V., Devedjian, J.C., Duce, J.A., Pradat, P.F., 2019. A ferroptosis-based panel of prognostic biomarkers for. Amyotrophic Lateral Sclerosis. Sci Rep 9 (1), 2918. doi:10.1038/s41598-019-39739-5.

Dickie, E.W., Anticevic, A., Smith, D.E., Coalson, T.S., Manogaran, M., Calarco, N., Viviano, J.D., Glasser, M.F., Van Essen, D.C., Voineskos, A.N, 2019. Ciftify: A framework for surface-based analysis of legacy MR acquisitions. NeuroImage 197, 818–826. doi:10.1016/j.neuroimage.2019.04.078.

Dukic, S., McMackin, R., Buxo, T., Fasano, A., Chipika, R., Pinto-Grau, M., Costello, E., Schuster, C., Hammond, M., Heverin, M., Coffey, A., Broderick, M., Iyer, P.M., Mohr, K., Gavin, B., Pender, N., Bede, P., Muthuraman, M., Lalor, E.C., Hardiman, O., Nasseroleslami, B., 2019. Patterned functional network disruption in amyotrophic lateral sclerosis. Hum Brain Mapp 40 (16), 4827–4842. doi:10.1002/hbm.24740.

Echaniz-Laguna, A., Rousso, E., Anheim, M., Fleury, M., Cossée, M., Tranchant, C., 2005. A clinical, neurophysiological and molecular study of 12 patients from 4 families with spinal and bulbar muscular atrophy. Revue neurologique 161 (4), 437–444. doi:10.1016/s0035-3787(05)85073-8.

Elamin, M., Bede, P., Montuschi, A., Pender, N., Chio, A., Hardiman, O., 2015. Predicting prognosis in amyotrophic lateral sclerosis: a simple algorithm. J Neurol 262 (6), 1447–1454. doi:10.1007/s00415-015-7731-6.

Ferraro, P.M., Agosta, F., Riva, N., Copetti, M., Spinelli, E.G., Falzone, Y., Sorarù, G., Comi, G., Chiò, A., Filippi, M., 2017. Multimodal structural MRI in the diagnosis of motor neuron diseases. NeuroImage: Clinical 16, 240–247. doi:10.1016/j.nicl.2017.08.002.

Finegan, E., Chipika, R.H., Li Hi Shing, S., Doherty, M.A., Hengeveld, J.C., Vajda, A., Donaghy, C., McLaughlin, R.L., Pender, N., Hardiman, O., Bede, P., 2019a. The clinical and radiological profile of primary lateral sclerosis: a population-based study. J Neurol 266 (11), 2718–2733. doi:10.1007/s00415-019-09473-z.

Finegan, E., Chipika, R.H., Shing, S.L.H., Hardiman, O., Bede, P., 2019b. Primary lateral sclerosis: a distinct entity or part of the ALS spectrum? Amyotroph Lateral Scler Frontotemporal Degener 20 (3-4), 133–145. doi:10.1080/21678421.2018.1550518.

Finegan, E., Hi Shing, S.L., Chipika, R.H., McKenna, M.C., Doherty, M.A., Hengeveld, J.C., Vajda, A., Donaghy, C., McLaughlin, R.L., Hutchinson, S., Hardiman, O., Bede, P., 2020. Thalamic, hippocampal and basal ganglia pathology in primary lateral sclerosis and amyotrophic lateral sclerosis: evidence from quantitative imaging data. Data Brief 29, 105115. doi:10.1016/j.dib.2020.105115.

Finegan, E., Li Hi Shing, S., Chipika, R.H., Doherty, M.A., Hengeveld, J.C., Vajda, A., Donaghy, C., Pender, N., McLaughlin, R.L., Hardiman, O., Bede, P., 2019c. Widespread subcortical grey matter degeneration in primary lateral sclerosis: a multimodal imaging study with genetic profiling. NeuroImage Clinical 24, 102089. doi:10.1016/j.nicl.2019.102089.

Finegan, E., Li Hi Shing, S., Siah, W.F., Chipika, R.H., Chang, K.M., McKenna, M.C., Doherty, M.A., Hengeveld, J.C., Vajda, A., Donaghy, C., Hutchinson, S., McLaughlin, R.L., Hardiman, O., Bede, P., 2020a. Evolving diagnostic criteria in primary lateral sclerosis: the clinical and radiological basis of "probable PLS. J Neurol Sci 417, 117052. doi:10.1016/j.jns.2020.117052.

Finegan, E., Shing, S.L.H., Chipika, R.H., Chang, K.M., McKenna, M.C., Doherty, M.A., Hengeveld, J.C., Vajda, A., Pender, N., Donaghy, C., Hutchinson, S., McLaughlin, R.L., Hardiman, O., Bede, P., 2021. Extra-motor cerebral changes and manifestations in primary lateral sclerosis. Brain Imaging Behav doi:10.1007/s11682-020-00421-4.

Finegan, E., Siah, W.F., Shing, S.L.H., Chipika, R.H., Chang, K.M., McKenna, M.C., Doherty, M.A., Hengeveld, J.C., Vajda, A., Donaghy, C., Hutchinson, S., McLaughlin, R.L., Hardiman, O., Bede, P., 2020b. Imaging and clinical data indicate considerable disease burden in 'probable' PLS: patients with UMN symptoms for 2-4 years. Data Brief, 106247 doi:10.1016/j.dib.2020.106247.

Fischl, B., 2012. FreeSurfer. NeuroImage 62 (2), 774–781. doi:10.1016/j.neuroimage.2012.01.021.

Gaser, C., Schlaug, G., 2003. Brain structures differ between musicians and non-musicians. J Neurosci 23 (27), 9240–9245. doi:10.1523/jneurosci.23-27-09240.2003.

Gordon, P.H., Cheng, B., Katz, I.B., Pinto, M., Hays, A.P., Mitsumoto, H., Rowland, L.P, 2006. The natural history of primary lateral sclerosis. Neurology 66 (5), 647–653.

Grollemund, V., Chat, G.L., Secchi-Buhour, M.S., Delbot, F., Pradat-Peyre, J.F., Bede, P., Pradat, P.F., 2020a. Development and validation of a 1-year survival prognosis estimation model for amyotrophic lateral sclerosis using manifold learning algorithm UMAP. Sci Rep 10 (1), 13378. doi:10.1038/s41598-020-70125-8.

Grollemund, V., Le Chat, G., Secchi-Buhour, M.S., Delbot, F., Pradat-Peyre, J.F., Bede, P., Pradat, P.F., 2020b. Manifold learning for amyotrophic lateral sclerosis functional loss assessment : development and validation of a prognosis model. J Neurol doi:10.1007/s00415-020-10181-2.

Grollemund, V., Pradat, P.F., Querin, G., Delbot, F., Le Chat, G., Pradat-Peyre, J.F., Bede, P., 2019. Machine learning in amyotrophic lateral sclerosis: achievements, pitfalls, and future directions. Front Neurosci 13, 135. doi:10.3389/fnins.2019.00135.

Hardiman, O., Doherty, C.P., Elamin, M., Bede, P., 2016. Neurodegenerative Disorders: A Clinical Guide, 2016 ed Springer International Publishing, Springer Cham Heidelberg New York Dordrecht London© Springer International Publishing, Switzerland 2016.

Hudziak, J.J., Albaugh, M.D., Ducharme, S., Karama, S., Spottswood, M., Crehan, E., Evans, A.C., Botteron, K.N, 2014. Cortical thickness maturation and duration of music training: health-promoting activities shape brain development. J Am Acad Child Adolesc Psychiatry 53 (11), 1153–1161. doi:10.1016/j.jaac.2014.06.015.

Ince, P.G., Evans, J., Knopp, M., Forster, G., Hamdalla, H.H., Wharton, S.B., Shaw, P.J, 2003. Corticospinal tract degeneration in the progressive muscular atrophy variant of ALS. Neurology 60 (8), 1252–1258. doi:10.1212/01.wnl.0000058901.75728.4e.

Kassubek, J., Juengling, F.D., Sperfeld, A.D, 2007. Widespread white matter changes in Kennedy disease: a voxel based morphometry study. J. Neurol. Neurosurg. Psychiatry 78 (11), 1209–1212. doi:10.1136/jnnp.2006.112532.

Kiernan, J.A., Hudson, A.J, 1994. Frontal lobe atrophy in motor neuron diseases. Brain 117 (Pt 4), 747–757.

Lai, T.H., Liu, R.S., Yang, B.H., Wang, P.S., Lin, K.P., Lee, Y.C., Soong, B.W, 2013. Cerebral involvement in spinal and bulbar muscular atrophy (Kennedy's disease): a pilot study of PET. J Neurol Sci 335 (1-2), 139–144. doi:10.1016/j.jns.2013.09.016.

Lazar, S.W., Kerr, C.E., Wasserman, R.H., Gray, J.R., Greve, D.N., Treadway, M.T., McGarvey, M., Quinn, B.T., Dusek, J.A., Benson, H., Rauch, S.L., Moore, C.I., Fischl, B., 2005. Meditation experience is associated with increased cortical thickness. Neuroreport 16 (17), 1893–1897. doi:10.1097/01.wnr.0000186598.66243.19.

Lebouteux, M.V., Franques, J., Guillevin, R., Delmont, E., Lenglet, T., Bede, P., Desnuelle, C., Pouget, J., Pascal-Mousselard, H., Pradat, P.F, 2014. Revisiting the spectrum of lower motor neuron diseases with snake eyes appearance on magnetic resonance imaging. Eur J Neurol 21 (9), 1233–1241. doi:10.1111/ene.12465.

Li Hi Shing, S., Chipika, R.H., Finegan, E., Murray, D., Hardiman, O., Bede, P., 2019. Post-polio syndrome: more than just a lower motor neuron disease. Front Neurol 10, 773. doi:10.3389/fneur.2019.00773.

Li Hi Shing, S., Lope, J., Chipika, R.H., Hardiman, O., Bede, P., 2021. Extra-motor manifestations in post-polio syndrome (PPS): fatigue, cognitive symptoms and radiological features. Neurol Sci doi:10.1007/s10072-021-05130-4.

Li Hi Shing, S., Lope, J., McKenna, M.C., Chipika, R.H., Hardiman, O., Bede, P., 2021. Increased cerebral integrity metrics in poliomyelitis survivors: putative adaptation to longstanding lower motor neuron degeneration. J Neurol Sci, 117361 doi:10.1016/j.jns.2021.117361.

Losito, L., Gennaro, L., Lucarelli, E., Trabacca, A., 2020. Brain MRI abnormalities in a child with spinal muscular atrophy type II. Acta neurologica Belgica doi:10.1007/s13760-020-01524-x.

Mackenzie, I.R.A., Briemberg, H., 2020. TDP-43 pathology in primary lateral sclerosis. Amyotroph Lateral Scler Frontotemporal Degener 1–7. doi:10.1080/21678421.2020.1790607.

Meier, J.M., van der Burgh, H.K., Nitert, A.D., Bede, P., de Lange, S.C., Hardiman, O., van den Berg, L.H., van den Heuvel, M.P., 2020. Connectome-based propagation model in amyotrophic lateral sclerosis. Ann Neurol 87 (5), 725–738. doi:10.1002/ana.25706.

Mendonça, R.H., Rocha, A.J., Lozano-Arango, A., Diaz, A.B., Castiglioni, C., Silva, A.M.S., Reed, U.C., Kulikowski, L., Paramonov, I., Cuscó, I., Tizzano, E.F., Zanoteli, E., 2019. Severe brain involvement in 5q spinal muscular atrophy type 0. Ann Neurol 86 (3), 458–462. doi:10.1002/ana.25549.

Menke, R.A.L., Proudfoot, M., Talbot, K., Turner, M.R, 2018. The two-year progression of st7ructural and functional cerebral MRI in amyotrophic lateral sclerosis. NeuroImage: Clinical 17, 953–961. doi:10.1016/j.nicl.2017.12.025.

Mitsumoto, H., Ulug, A.M., Pullman, S.L., Gooch, C.L., Chan, S., Tang, M.X., Mao, X., Hays, A.P., Floyd, A.G., Battista, V., Montes, J., Hayes, S., Dashnaw, S., Kaufmann, P., Gordon, P.H., Hirsch, J., Levin, B., Rowland, L.P., Shungu, D.C, 2007. Quantitative objective markers for upper and lower motor neuron dysfunction in ALS. Neurology 68 (17), 1402–1410. doi:10.1212/01.wnl.0000260065.57832.87.

Müller, H.P., Del Tredici, K., Lulé, D., Müller, K., Weishaupt, J.H., Ludolph, A.C., Kassubek, J., 2020. vivo histopathological staging in C9orf72-associated ALS: A tract of interest DTI study. NeuroImage Clinical 27, 102298. doi:10.1016/j.nicl.2020.102298.

Müller, H.P., Gorges, M., Kassubek, R., Dorst, J., Ludolph, A.C., Kassubek, J., 2018. Identical patterns of cortico-efferent tract involvement in primary lateral sclerosis and amyotrophic lateral sclerosis: a tract of interest-based MRI study. NeuroImage: Clinical 18, 762–769. doi:10.1016/j.nicl.2018.03.018.

Muller, H.P., Turner, M.R., Grosskreutz, J., Abrahams, S., Bede, P., Govind, V., Prudlo, J., Ludolph, A.C., Filippi, M., Kassubek, J., 2016. A large-scale multicentre cerebral diffusion tensor imaging study in amyotrophic lateral sclerosis. J. Neurol. Neurosurg. Psychiatry 87 (6), 570–579. doi:10.1136/jnnp-2015-311952.

Muller, H.P., Unrath, A., Huppertz, H.J., Ludolph, A.C., Kassubek, J., 2012. Neuroanatomical patterns of cerebral white matter involvement in different motor neuron diseases as studied by diffusion tensor imaging analysis. Amyotroph Lateral Scler 13 (3), 254–264. doi:10.3109/17482968.2011.653571.

Nasseroleslami, B., Dukic, S., Broderick, M., Mohr, K., Schuster, C., Gavin, B., McLaughlin, R., Heverin, M., Vajda, A., Iyer, P.M., Pender, N., Bede, P., Lalor, E.C., Hardiman, O., 2019. Characteristic increases in EEG connectivity correlate with changes of structural MRI in amyotrophic lateral sclerosis. Cereb Cortex 29 (1), 27–41. doi:10.1093/cercor/bhx301.

Nelles, M., Block, W., Traber, F., Wullner, U., Schild, H.H., Urbach, H., 2008. Combined 3T diffusion tensor tractography and 1H-MR spectroscopy in motor neuron disease. AJNR Am J Neuroradiol 29 (9), 1708–1714.

Nishimura, Y., Isa, T., 2009. Compensatory changes at the cerebral cortical level after spinal cord injury. The Neuroscientist : a review journal bringing neurobiology. Neurol Psychiatr 15 (5), 436–444. doi:10.1177/1073858408331375.

Pereira, A.C., Huddleston, D.E., Brickman, A.M., Sosunov, A.A., Hen, R., McKhann, G.M., Sloan, R., Gage, F.H., Brown, T.R., Small, S.A, 2007. An in vivo correlate of exercise-induced neurogenesis in the adult dentate gyrus. Proc Natl Acad Sci U S A 104 (13), 5638–5643. doi:10.1073/pnas.0611721104.

Pieper, C.C., Konrad, C., Sommer, J., Teismann, I., Schiffbauer, H., 2013. Structural changes of central white matter tracts in Kennedy's disease - a diffusion tensor imaging and voxel-based morphometry study. Acta Neurol Scand 127 (5), 323–328. doi:10.1111/ane.12018.

Pinheiro, J., Bates, D., DebRoy, S., Sarkar, D., Team, R.C. 2020. nlme: Linear and nonlinear mixed effects models. R package version 3.1-150. Accessed from: https://cran.r-project.org/web/packages/nlme/index.html, (Accessed on 10/10/2021).

Pioro, E.P., Turner, M.R., Bede, P., 2020. Neuroimaging in primary lateral sclerosis. Amyotroph Lateral Scler Frontotemporal Degener 21 (sup1), 18–27. doi:10.1080/21678421.2020.1837176.

Proudfoot, M., Bede, P., Turner, M.R, 2018. Imaging cerebral activity in amyotrophic lateral sclerosis. Front Neurol 9, 1148. doi:10.3389/fneur.2018.01148.

Prudlo, J., Bißbort, C., Glass, A., Grossmann, A., Hauenstein, K., Benecke, R., Teipel, S.J, 2012. White matter pathology in ALS and lower motor neuron ALS variants: a diffusion tensor imaging study using tract-based spatial statistics. J Neurol 259 (9), 1848–1859. doi:10.1007/s00415-012-6420-y.

Querin, G., Bede, P., El Mendili, M.M., Li, M., Pelegrini-Issac, M., Rinaldi, D., Catala, M., Saracino, D., Salachas, F., Camuzat, A., Marchand-Pauvert, V., Cohen-Adad, J., Colliot, O., Le Ber, I., Pradat, P.F., 2019a. Presymptomatic spinal cord pathology in c9orf72 mutation carriers: a longitudinal neuroimaging study. Ann Neurol 86 (2), 158–167. doi:10.1002/ana.25520.

Querin, G., Bede, P., Marchand-Pauvert, V., Pradat, P.F, 2018a. Biomarkers of spinal and bulbar muscle atrophy (SBMA): a comprehensive review. Front Neurol 9, 844. doi:10.3389/fneur.2018.00844.

Querin, G., El Mendili, M.M., Bede, P., Delphine, S., Lenglet, T., Marchand-Pauvert, V., Pradat, P.F., 2018b. Multimodal spinal cord MRI offers accurate diagnostic classification in ALS. J. Neurol. Neurosurg. Psychiatry 89 (11), 1220–1221. doi:10.1136/jnnp-2017-317214.

Querin, G., El Mendili, M.M., Lenglet, T., Behin, A., Stojkovic, T., Salachas, F., Devos, D., Le Forestier, N., Del Mar Amador, M., Debs, R., Lacomblez, L., Meninger, V., Bruneteau, G., Cohen-Adad, J., Lehericy, S., Laforet, P., Blancho, S., Benali, H., Catala, M., Li, M., Marchand-Pauvert, V., Hogrel, J.Y., Bede, P., Pradat, P.F., 2019b. The spinal and cerebral profile of adult spinal-muscular atrophy: a multimodal imaging study. NeuroImage Clinical 21, 101618. doi:10.1016/j.nicl.2018.101618.

Querin, G., Lenglet, T., Debs, R., Stojkovic, T., Behin, A., Salachas, F., Le Forestier, N., Amador, M.D.M., Lacomblez, L., Meininger, V., Bruneteau, G., Laforet, P., Blancho, S., Marchand-Pauvert, V., Bede, P., Hogrel, J.Y., Pradat, P.F, 2018c. The motor unit number index (MUNIX) profile of patients with adult spinal muscular atrophy. Clin Neurophysiol 129 (11), 2333–2340. doi:10.1016/j.clinph.2018.08.025.

Raaphorst, J., van Tol, M.J., Groot, P.F., Altena, E., van der Werf, Y.D., Majoie, C.B., van der Kooi, A.J., van den Berg, L.H., Schmand, B., de Visser, M., Veltman, D.J, 2014. Prefrontal involvement related to cognitive impairment in progressive muscular atrophy. Neurology 83 (9), 818–825. doi:10.1212/wnl.0000000000000745.

Sale, M.V., Reid, L.B., Cocchi, L., Pagnozzi, A.M., Rose, S.E., Mattingley, J.B, 2017. Brain changes following four weeks of unimanual motor training: evidence from behavior, neural stimulation, cortical thickness, and functional MRI. Hum Brain Mapp 38 (9), 4773–4787. doi:10.1002/hbm.23710.

Salimi-Khorshidi, G., Smith, S.M., Nichols, T.E, 2011. Adjusting the effect of nonstationarity in cluster-based and TFCE inference. NeuroImage 54 (3), 2006–2019. doi:10.1016/j.neuroimage.2010.09.088.

Schaefer, A., Kong, R., Gordon, E.M., Laumann, T.O., Zuo, X.N., Holmes, A.J., Eickhoff, S.B., Yeo, B.T.T, 2018. Local-global parcellation of the human cerebral cortex from intrinsic functional connectivity MRI. Cereb Cortex 28 (9), 3095–3114. doi:10.1093/cercor/bhx179.

Schuster, C., Elamin, M., Hardiman, O., Bede, P., 2015. Presymptomatic and longitudinal neuroimaging in neurodegeneration–from snapshots to motion picture: a systematic review. J. Neurol. Neurosurg. Psychiatry 86 (10), 1089–1096. doi:10.1136/jnnp-2014-309888.

Schuster, C., Hardiman, O., Bede, P., 2016. Development of an automated MRI-based diagnostic protocol for amyotrophic lateral sclerosis using disease-specific pathognomonic features: a quantitative disease-state classification study. PLoS One 11 (12), e0167331. doi:10.1371/journal.pone.0167331.

Schuster, C., Hardiman, O., Bede, P., 2017. Survival prediction in amyotrophic lateral sclerosis based on MRI measures and clinical characteristics. BMC Neurol 17 (1), 73. doi:10.1186/s12883-017-0854-x.

Shafto, M.A., Tyler, L.K., Dixon, M., Taylor, J.R., Rowe, J.B., Cusack, R., Calder, A.J., Marslen-Wilson, W.D., Duncan, J., Dalgleish, T., Henson, R.N., Brayne, C., Matthews, F.E, 2014. The Cambridge centre for ageing and neuroscience (Cam-CAN) study protocol: a cross-sectional, lifespan, multidisciplinary examination of healthy cognitive ageing. BMC Neurol 14, 204. doi:10.1186/s12883-014-0204-1.

Sperfeld, A.D., Bretschneider, V., Flaith, L., Unrath, A., Hanemann, C.O., Ludolph, A.C., Kassubek, J., 2005. MR-pathologic comparison of the upper spinal cord in different motor neuron diseases. Eur Neurol 53 (2), 74–77. doi:10.1159/000084650.

Spinelli, E.G., Agosta, F., Ferraro, P.M., Querin, G., Riva, N., Bertolin, C., Martinelli, I., Lunetta, C., Fontana, A., Sorarù, G., Filippi, M., 2019. Brain MRI shows white matter sparing in Kennedy's disease and slow-progressing lower motor neuron disease. Hum Brain Mapp 40 (10), 3102–3112. doi:10.1002/hbm.24583.

Sterr, A., Dean, P.J., Vieira, G., Conforto, A.B., Shen, S., Sato, J.R, 2013. Cortical thickness changes in the non-lesioned hemisphere associated with non-paretic arm immobilization in modified CI therapy. NeuroImage Clinical 2, 797–803. doi:10.1016/j.nicl.2013.05.005.

Tahedl, M., 2020. Towards individualized cortical thickness assessment for clinical routine. J Transl Med 18 (1), 151. doi:10.1186/s12967-020-02317-9.

Tahedl, M., Chipika, R.H., Lope, J., Li Hi Shing, S., Hardiman, O., Bede, P., 2021. Cortical progression patterns in individual ALS patients across multiple timepoints: a mosaic-based approach for clinical use. J Neurol doi:10.1007/s00415-020-10368-7.

Thomas, A.G., Dennis, A., Rawlings, N.B., Stagg, C.J., Matthews, L., Morris, M., Kolind, S.H., Foxley, S., Jenkinson, M., Nichols, T.E., Dawes, H., Bandettini, P.A., Johansen-Berg, H., 2016. Multi-modal characterization of rapid anterior hippocampal volume increase associated with aerobic exercise. NeuroImage 131, 162–170. doi:10.1016/j.neuroimage.2015.10.090.

Turner, M.R., Barohn, R.J., Corcia, P., Fink, J.K., Harms, M.B., Kiernan, M.C., Ravits, J., Silani, V., Simmons, Z., Statland, J., van den Berg, L.H., Mitsumoto, H., 2020. Primary lateral sclerosis: consensus diagnostic criteria. J. Neurol. Neurosurg. Psychiatry 91 (4), 373–377. doi:10.1136/jnnp-2019-322541.

Unrath, A., Muller, H.P., Riecker, A., Ludolph, A.C., Sperfeld, A.D., Kassubek, J., 2010. Whole brain-based analysis of regional white matter tract alterations in rare motor neuron diseases by diffusion tensor imaging. Hum Brain Mapp 31 (11), 1727–1740. doi:10.1002/hbm.20971.

van der Burgh, H.K., Westeneng, H.J., Meier, J.M., van Es, M.A., Veldink, J.H., Hendrikse, J., van den Heuvel, M.P., van den Berg, L.H., 2019. Cross-sectional and longitudinal assessment of the upper cervical spinal cord in motor neuron disease. NeuroImage Clinical 24, 101984. doi:10.1016/j.nicl.2019.101984.

van der Graaff, M.M., Lavini, C., Akkerman, E.M., Majoie Ch, B., Nederveen, A.J., Zwinderman, A.H., Brugman, F., van den Berg, L.H., de Jong, J.M., de Visser, M., 2010. MR spectroscopy findings in early stages of motor neuron disease. AJNR Am J Neuroradiol 31 (10), 1799–1806.

van der Graaff, M.M., Sage, C.A., Caan, M.W., Akkerman, E.M., Lavini, C., Majoie, C.B., Nederveen, A.J., Zwinderman, A.H., Vos, F., Brugman, F., van den Berg, L.H., de Rijk, M.C., van Doorn, P.A., Van Hecke, W., Peeters, R.R., Robberecht, W., Sunaert, S., de Visser, M., 2011a. Upper and extra-motoneuron involvement in early motoneuron disease: a diffusion tensor imaging study. Brain : a J Neurol 134 (Pt 4), 1211–1228. doi:10.1093/brain/awr016.

Van Der Graaff, M.M., Sage, C.A., Caan, M.W.A., Akkerman, E.M., Lavini, C., Majoie, C.B., Nederveen, A.J., Zwinderman, A.H., Vos, F., Brugman, F., Van Den Berg, L.H., De Rijk, M.C., Van Doorn, P.A., Van Hecke, W., Peeters, R.R., Robberecht, W., Sunaert, S., De Visser, M, 2011b. Upper and extra-motoneuron involvement in early motoneuron disease: a diffusion tensor imaging study. Brain : a J Neurol 134 (4), 1211–1228. doi:10.1093/brain/awr016.

Van Essen, D.C., Smith, S.M., Barch, D.M., Behrens, T.E.J., Yacoub, E., Ugurbil, K., 2013. The WU-Minn human connectome project: an overview. NeuroImage 80, 62–79. doi:10.1016/j.neuroimage.2013.05.041.

Verstraete, E., Turner, M.R., Grosskreutz, J., Filippi, M., Benatar, M., 2015. Mind the gap: the mismatch between clinical and imaging metrics in ALS. Amyotroph Lateral Scler Frontotemporal Degener 16 (7-8), 524–529. doi:10.3109/21678421.2015.1051989.

Welsh, R.C., Jelsone-Swain, L.M., Foerster, B.R, 2013. The utility of independent component analysis and machine learning in the identification of the amyotrophic lateral sclerosis diseased brain. Front Hum Neurosci 7, 251. doi:10.3389/fnhum.2013.00251.

Westeneng, H.J., Debray, T.P.A., Visser, A.E., van Eijk, R.P.A., Rooney, J.P.K., Calvo, A., Martin, S., McDermott, C.J., Thompson, A.G., Pinto, S., Kobeleva, X., Rosenbohm, A., Stubendorff, B., Sommer, H., Middelkoop, B.M., Dekker, A.M., van Vugt, J., van Rheenen, W., Vajda, A., Heverin, M., Kazoka, M., Hollinger, H., Gromicho, M., Korner, S., Ringer, T.M., Rodiger, A., Gunkel, A., Shaw, C.E., Bredenoord, A.L., van Es, M.A., Corcia, P., Couratier, P., Weber, M., Grosskreutz, J., Ludolph, A.C., Petri, S., de Carvalho, M., Van Damme, P., Talbot, K., Turner, M.R., Shaw, P.J., Al-Chalabi, A., Chio, A., Hardiman, O., Moons, K.G.M., Veldink, J.H., van den Berg, L.H., 2018. Prognosis for patients with amyotrophic lateral sclerosis: development and validation of a personalised prediction model. Lancet Neurol doi:10.1016/s1474-4422(18)30089-9.

Winkler, A.M., Ridgway, G.R., Webster, M.A., Smith, S.M., Nichols, T.E, 2014. Permutation inference for the general linear model. NeuroImage 92, 381–397. doi:10.1016/j.neuroimage.2014.01.060.

Yeo, B.T., Krienen, F.M., Sepulcre, J., Sabuncu, M.R., Lashkari, D., Hollinshead, M., Roffman, J.L., Smoller, J.W., Zöllei, L., Polimeni, J.R., Fischl, B., Liu, H., Buckner, R.L, 2011. The organization of the human cerebral cortex estimated by intrinsic functional connectivity. J Neurophysiol 106 (3), 1125–1165. doi:10.1152/jn.00338.2011.

Yunusova, Y., Plowman, E.K., Green, J.R., Barnett, C., Bede, P., 2019. Clinical measures of bulbar dysfunction in ALS. Front Neurol 10, 106. doi:10.3389/fneur.2019.00106.